Eurographics Symposium on Rendering 2017
P. Sander and M. Zwicker
(Guest Editors)

Volume 36 (2017), Number 4

An Appearance Model for Textile Fibers

Carlos Aliaga[1] Carlos Castillo[2] Diego Gutierrez[1] Miguel A. Otaduy[2] Jorge Lopez-Moreno[2] Adrian Jarabo[1]

[1]Universidad de Zaragoza, I3A [2]Universidad Rey Juan Carlos

Figure 1: *Volumetric rendering of three fabric samples using our highly-detailed physically-based BCSDFs models. Our model is based on the optical and structural parameters particular of each cloth fiber. From left to right, a 2-ply knitted garter (7 twist/cm, 120 fibers/yarn) of cotton fibers, a single-ply woven satin made of silk (1 twist/cm, 30 fibers/yarn) and a 2-ply knitted garter (4 twist/cm, 160 fibers/yarn) made of polyester fibers. Silk and cotton pieces are colored with reactive dyes, and a disperse dye is used for polyester.*

Abstract

Accurately modeling how light interacts with cloth is challenging, due to the volumetric nature of cloth appearance and its multiscale structure, where microstructures play a major role in the overall appearance at higher scales. Recently, significant effort has been put on developing better microscopic models for cloth structure, which have allowed rendering fabrics with unprecedented fidelity. However, these highly-detailed representations still make severe simplifications on the scattering by individual fibers forming the cloth, ignoring the impact of fibers' shape, and avoiding to establish connections between the fibers' appearance and their optical and fabrication parameters. In this work we put our focus in the scattering of individual cloth fibers; we introduce a physically-based scattering model for fibers based on their low-level optical and geometric properties, relying on the extensive textile literature for accurate data. We demonstrate that scattering from cloth fibers exhibits much more complexity than current fiber models, showing important differences between cloth type, even in averaged conditions due to longer views. Our model can be plugged in any framework for cloth rendering, matches scattering measurements from real yarns, and is based on actual parameters used in the textile industry, allowing predictive bottom-up definition of cloth appearance.

CCS Concepts

•***Computing methodologies*** → ***Fiber Scattering;*** *Appearance Modeling; Cloth Rendering;*

1. Introduction

Rendering realistic fabrics is an active research field in computer graphics, with many applications in other areas like entertainment or textile design. Accurately reproducing the appearance of cloth remains challenging, due to the micro-structures found at fiber level, and the complex light scattering patterns exhibited at such scales. This affects the overall look of cloth both in close-ups, and at longer viewing distances, with effects like anisotropic specular highlights, or anisotropic multiple scattering.

Given this intrinsic complexity, and the effect of microscale appearance at coarser scales, it is necessary to accurately represent appearance at very small scales, to capture the subtleties and rich optical phenomena of cloth fibers. Recent approaches have made significant advances in this direction, either by modeling the ar-

rangement of the fibers [SKZ11], or capturing the structure of small pieces of cloth using macro photographs [SZK15] or Computed Tomography scanners (CT) [ZJMB11, KSZ*15, ZLB16]. However, these works focus on reconstructing the geometry of the fibers, while adopting several convenient simplifications to simulate the scattering of light, such as using parametric, simplified fiber scattering models. While these models improve over general volumetric phase functions such as microflakes when rendering cloth [KSZ*15], they 1) still rely on very simplified models of fibers, and 2) lack the actual fabrication parameters used when physically manufacturing the fiber. These two points limit the applicability of current models for predictive rendering, based on optimization-based approaches.

In this paper we introduce a novel appearance model for cloth, focusing on high-quality scattering functions, which takes into account the optical and structural properties of real-world cloth fibers, from a ray-optics perspective. We leverage the wealth of measured, real-world data available from the textile research community, and build digital replicas of different types of fibers (polyester, wool, silk and cotton). We then rely on brute force simulations of light scattering of such fibers to obtain highly detailed tabulated *Bidirectional Curve Scattering Distribution Functions (BCSDF)*, without the most common simplifications assumed in current BCSDF models [ZW07, KM16] (e.g. circular or elliptical cross sections), which are unable to capture the rich visual features of real fibers. Moreover, since our model is based on low-level real-world fiber properties, it allows us to specify actual fabrication parameters used by fiber makers; this is very relevant in fields such as textile or cloth design, where manual or optimization-based parameters fitting might not match the properties of actual existing fibers. To our knowledge, ours is the first scattering model based on such physical and optical measurements, including fibers' index of refraction, surface roughness and dye concentration.

We compare our model against state-of-the-art BCSDFs at different scales: at highly detailed close-up views where the scattering of individual fibers is visible, as well as at longer shots where the scattering of the individual fibers is averaged, and the macroscopic appearance of cloth becomes clear. Our BCSDFs can be directly used for rendering both volumetric-based (see e.g. Figure 1) and explicit fiber-based representations of cloth; moreover, since it allows for a bottom-up definition of cloth appearance, it bridges the gap between actual fiber fabrication parameters and simulated cloth appearance in a predictive manner.

2. Related Work

We focus on detailed volumetric or explicit representations of cloth appearance, although other approaches using planar representations of cloth exist, based either in bidirectional texture functions (BTFs) [DVGNK99, SSK03] or in parametric local scattering models [IM12, SBdDJ13]. For more details we refer to the original papers, or the survey by Schröder and colleagues [SZZ12].

Volumetric cloth modeling Two different approaches for volumetric cloth representation have been widely adopted in the field: 1) assuming cloth as an heterogeneous anisotropic volume [JAM*10] and posing the rendering problem as volumetric light transport, and 2) modeling the geometry of each yarn or fiber explicitly, similar to recent hair rendering approaches.

Zhao and colleagues [ZJMB11] followed the former approach, leveraging Micro-CT scanners of cloth in order to obtain highly detailed volumes at micron resolution of small pieces of fabric. Micro-CTs have also been used as building blocks for larger garments with repeated patterns [ZJMB12], and to take advantage of the repeated structure of cloth to precompute inter-blocks light transport to accelerate rendering [ZHRB13]. While CT-based models allow for high-quality renders of cloth, they rely in complex and expensive capturing setups, and manual intervention or optimization [KSZ*15] with respect to a target cloth appearance is needed to define the optical parameters of cloth garments. Instead of relying on captured data, Schröder and colleagues [SKZ11] procedurally generate cloth garments as a collection of individual yarns. These yarns are then transformed into a volumetric representation using Gaussian distributions of fiber orientation and density. Although such model can produce realistic results, it does not hold for close-up views where a huge number of voxels needs to be computed. Similarly, Lopez-Moreno et al. [LMMCO15] build a volumetric representation of cloth on the GPU. They adapt the classic *lumislice* algorithm [XCL*01] to interactively create high-quality volumetric representations of cloth at fiber scale.

As opposed to volumetric approaches, Schröder and colleagues [SZK15] relied on a fully geometrical representation of individual yarns, each with a different scattering function. They extended their previous work [SKZ11] entirely avoiding the volumetric representation of cloth. Their fully procedural fiber generation method even simulates the small fibers protruding from the yarn (hairiness) and allows predictive reverse engineering of real cloth. Zhao et al. [ZLB16] automated the fitting of such yarn procedural models from physical measurements acquired using micro CT imaging. Recently, Wu and Yuksel [WY17] demonstrated real-time rendering of cloth modeled using explicit yarns.

Despite their differences, both approaches (volumetric and explicit geometry) are able to deliver comparable high-quality results [KSZ*15]. Our work is orthogonal to the chosen cloth representation, and our realistic fiber-based scattering functions can be applied to both.

Finally, although not explicitly for cloth, we note that hybrid approaches considering volumetric and explicit representation of packed discrete media have been proposed, taking the best of each world by keeping the high-frequency details of explicit geometry in the first bounces, while accelerating rendering for higher-order scattering using a volumetric approximation [MPH*15, MPG*16].

Scattering models Most previous approaches have assumed general scattering models for fibers, ranging from microflakes [JAM*10, HDCD15] for volumetric models, to explicit fiber scattering models similar to hair rendering e.g. [KK89, MJC*03, ZW07, YTJR15].

While both extremes can produce visually realistic results, and many approaches have successfully used microflakes for rendering cloth [ZJMB11, ZHRB13, LMMCO15], it has been shown that microflakes cannot match the appearance of real-world cloth, while fiber scattering models are more suitable for this task [KSZ*15].

In this context, Schröder and colleagues [SKZ11, SZK15] use the parametric BCSDF model proposed by Zinke and Weber [ZW07]. Khungurn et al. [KSZ*15], on the other hand, proposed a simple fiber-based model suitable for both rendering and appearance capture of real garments. The authors highlight the importance of the fiber-specific scattering model to achieve good results, and choose a simplified BCSDF that fits well within their optimization framework. However, their fiber scattering model has certain limitations from a physical point of view, since it assumes only direct reflection and transmission, ignoring longer scattering orders within the fiber, and allowing colored reflectance which is not predicted in Fresnel's equations. The recent paper of Zhao et al. [ZLB16] relies on the same scattering model.

A common limitation shared by previous physically-based fiber scattering models [MJC*03, ZW07, dFH*11, YTJR15] and artist oriented models [SPJT10, CBTB16] is the lack of generality: they assume fibers are cylinders with a cross section that can be elliptical up to some degree. Ogaki et al. [OTS10] proposed a similar approach to ours for fur modeling, where explicit geometry was used to obtain hair scattering functions from fibers with arbitrary geometry. Their work, however, does not account for realistic fiber geometries based on Scanning Electron Microscope (SEM), and does not consider real-world measurements of optical parameters. The recent model by Khungurn and Marschner [KM16] is able to handle arbitrary eccentricity for the first time. However, fabric fibers lie far from this assumption (see Figure 2), leading to scattering patterns much more anisotropic and difficult to represent through current models. In addition, these models do not provide any connection between fabrication parameters and optical properties of the fibers; as we will show, these fabrication parameters have a major impact on the scattered field.

Textile Research Beyond computer graphics, several works in textile research have used simulation to predict the appearance of cloth. Most of these works use light simulation in yarns or fibers focusing on quality assessment of specific features such as luster [TMM09, AYMT03], and on determining the optical properties of cloth by means of inverse rendering [HSEMN09, RGS10]. Closer to our work, Yamada et al. [Yam02] compare through simulations the scattering functions of synthetic fibers with circular, triangular or rectangular cross sections. A similar approach is followed by Liu et al. [LW12] and Aslan et al. [AYMT02] for synthetic and cotton fibers respectively. None of these works use the computed scattering functions for rendering, nor propose a full bottom-up approach for defining cloth appearance. Finally, similar to other related work in graphics [ZJMB11, KSZ*15], Grasso et al. [GHR97] rely on simulation to study the effect of textile properties in the macroscopic appearance of cloth, while other works evaluate radiative transfer in fibers and textiles [YKTU92, MH99, YK00], and compare simulations and measurements of the propagation of polarized light through textile materials [PDW12]. These approaches focus either on a few properties individually, or on particular types of fiber, and do not attempt to provide a general model suitable for computer graphics. Instead, our model is capable of reproducing the appearance of cloth, based on fiber fabrication and measured optical parameters, making it well suited for predictive applications.

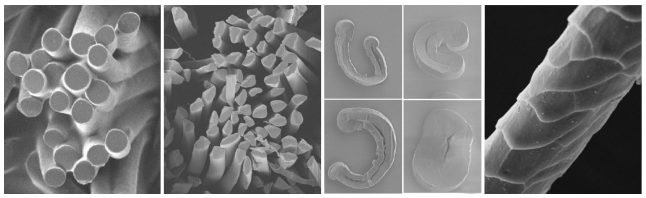

Figure 2: *SEM images of cross sections and shapes for real polyester, silk, cotton and wool fibers. Images from [DKP14], [SPV14], [NPH14] and [Kan07], respectively.*

3. Light Scattering from Textile Fibers

Most cloth fibers are made of an absorbing dielectric medium. Although their shape has been traditionally considered as a cylinder extruded from circular or elliptical cross sections, their actual cross sections greatly differ from these simplified shapes, depending on the type of fiber, as well as its chemical or mechanical treatment. Moreover, the assumption of a smooth cylindrical shape does not hold for some natural fibers such as wool, which presents overlapping, tilted scales on its surface (similar to human hair [MJC*03]). This can be seen in Figure 2, showing SEM samples of real textile fibers.

This leads to visually important reflectance features such as self occlusions or caustics, which cannot be simulated with current BCSDF [ZW07]. Figure 3 shows several examples of 2D slices of the four-dimensional BCSDF for different incoming directions ω_i (the coordinate system is described in Figure 4), computed for a set of fibers of polyester, silk, cotton and wool, each with different fiber cross sections and optical properties. While the BCSDF of polyester, a synthetic radially-symmetric fiber, is rotation-invariant and exhibits uniform high-frequency lobes due to sharp reflection and caustics on the cone of reflection, the rest of the natural fibers yield heterogeneous and highly anisotropic scattering profiles, dependent on the cross section and the incident light direction ω_i. Silk for instance exhibits sharp, highly anisotropic caustics due to its flat irregular shape. Cotton on the other hand presents wider lobes due to its higher surface roughness, its inside hole, and the multiple self-interreflections within the fiber boundaries, specially in the case of non-mercerized fibers. Finally, the reflectance of wool is more similar to perfect cylindrical fibers (e.g. polyester) due to the low eccentricity of its cross section, but presents a set of high-frequency anisotropies due to the irregular cuticle variation along the longitudinal axis.

In addition to structural properties, light scattering in a cloth fiber also depends on its optical properties, such as its index of refraction or the absorption, which in turn is highly dependent on the concentration of the dye used to color the fiber. Most previous work have attempted to model these parameters using a top-down approach, either by directly defining the fiber color [JAM*10, SKZ11], or matching a specific appearance through optimization [KSZ*15]. While this leads to visually plausible results, these approaches may lead to physically invalid parameters, such as absorption values out of the range of actual fabrics, or artifacts like colored specular reflections. Instead, we opt for a bottom-up approach, defining fiber

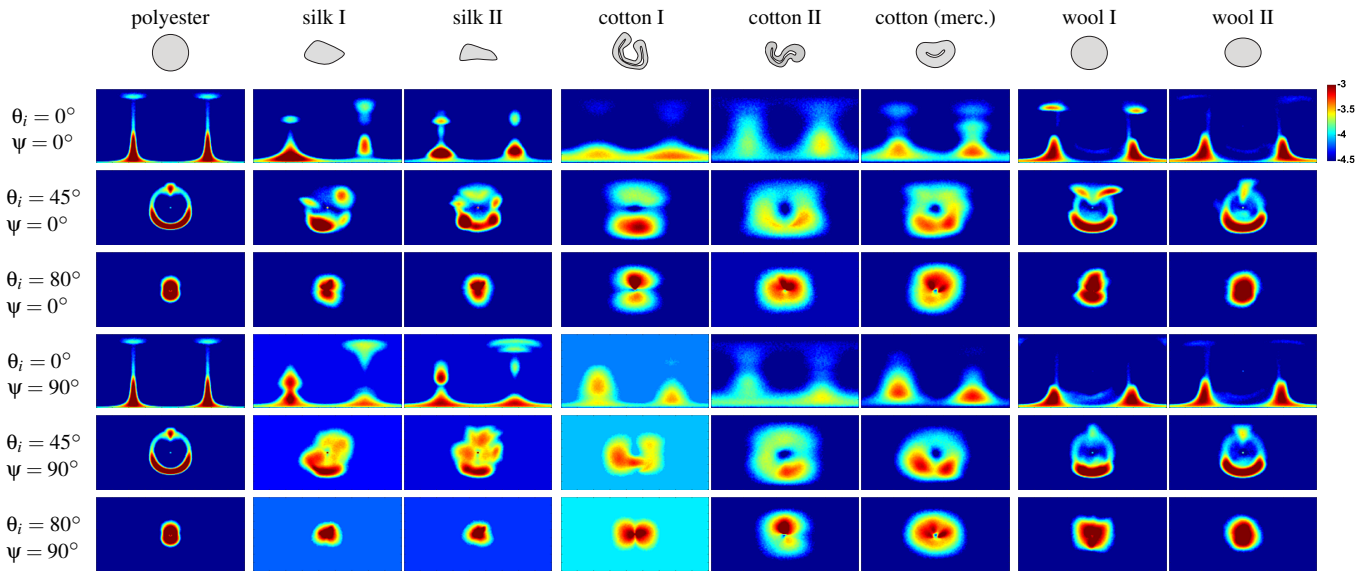

Figure 3: *Outgoing field of the BCSDF for a set of cloth fibers under varying illumination setups, with false color depicting radiance in logarithmic space. From left to right: polyester, silk, cotton and wool, each with several different cross sections (top), equalized in diameter for visualization purposes (real relative sizes can be found in Table 1). Each fiber is softly dyed ($\zeta = 0.1\%$). Note that the cross section of mercerised cotton, which is a typical treatment of this fiber to gain luster, is very different from untreated cotton. From top to bottom, the incident light varies from perpendicular direction to near grazing illumination angle $\theta_i = 0°, -45°, -80°$ respectively, and $\phi_i = 0°$, and the fiber is rotated along its tangent direction by $\psi = 0°$ and $90°$; see Figure 4 for the coordinates in the BCSDF.*

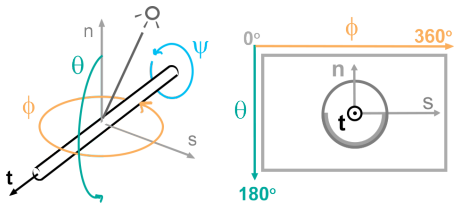

Figure 4: Left: *spherical coordinates and local frame defined for the fiber, aligned along the t axis.* Right: *illustration of coordinate system and shape of lobes observed in the scattering plots; circle in the middle is the reflection cone under illumination angle* $\theta_i = -45°$.

appearance from real-world low-level structural and chemical data, including the specific dyes used with different types of cloth.

Given this complexity, it is not feasible to derive an analytical BCSDF to simulate fiber appearance without major simplifications; instead, we follow previous works on modeling complex reflectance and appearance [SML*12, MPH*15, MPG*16], and build a tabulated BCSDF from a physically accurate fiber model, which takes into account precise structural and optical properties. This is described in detail in the following subsections, and compared against state-of-the-art fiber scattering models. Later we will show how to use these complex BCSDFs for rendering volumetric models of cloth.

Cross section and longitudinal structure To take into account how the different cross sections affect the optical properties of cloth, we analyzed SEM samples of real fibers, and manually modeled a representative set of different cross sections for each type. While some fibers such as polyester fit well into the assumption of cylindrical cross section, natural fibers present significant variability in their shapes, as we have seen. In addition, we also take into account the absolute size of each type of fiber; for instance, wool can be up to eight times larger in diameter than silk (see Table 1). Of all the fibers analyzed, wool presents an additional challenge: its surface is made up of overlapping cuticles (not present in other fibers, see Figure 2), which significantly affect light scattering. We approximate this effect by modeling shape variations along the longitudinal axis.

Type	Diameter μm	Density g/cm^3	IOR $\eta_{\parallel}, \eta_{\perp}$	$R_a\,(l)$ nm	β degrees
Polyester	10	1.39	1.73, 1.54	2.33-5 (30)	2.7-3.5
Silk	5-10	1.34	1.591, 1.538	8-9 (30)	6-7
Cotton	17-20	1.52	1.578, 1.532	12.5-15.8 (50)	14-17
Wool	24-40	1.31	1.553, 1.542	6 (50)	5

Table 1: *Measurements of the physical and optical properties of four of the most common fabrics, acquired from the textile literature: fiber diameters from Trotman [Tro84]; fiber densities (in a standard atmosphere of 65% relative humidity, 20^oC) and index of refraction from Hearle and Morton [HM08]; surface roughness R_a and l from [GK81, LXD08].*

3.1. Fiber properties

Surface roughness The dielectric boundaries of the fibers present roughness at nanoscopic scale, which prevents us from using directly the Fresnel equations (see index of refraction for all fibers

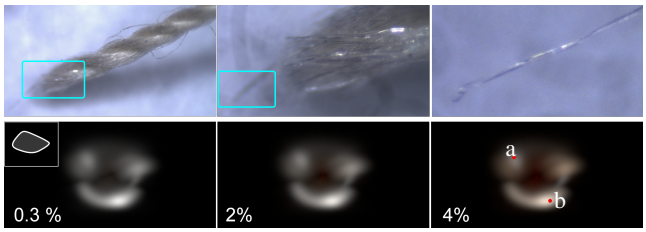

Figure 5: *Light absorption in fibers and threads. First row shows images under the microscope of a real silk thread of 3 plys, each composed by 90 fibers. The rightmost image shows how a single fiber has very low absorption, but the cumulative effect of each of the 90 fibers per ply give the thread its overall yellowish color. Second row shows the effect in our model of the DoS ζ used to dye the fibers, in particular, the scattering of a silk fiber (see cross section on the inset on the left) lit from $\omega_i = \langle 0^\circ, 45^\circ \rangle$ with an orange dye with a different ζ parameter: from left to right, it varies from very pale to very deep DoS (μ_a= 5.08, 40.46 and 84.68 mm^{-1}). While the reflection cone remains uncolored (specular reflection, (a) in the rightmost figure), it can be seen how the colored lobes increase in saturation when the amount of dye increases (b). Since the silk fibers are thin, note also that the refraction lobe remains softly colored even for deeply dyed fibers (right).*

in Table 1; note that the wavelength dependency on η is negligible [HM08]). As in recent work [DWMG15, NLW*16], we model surface roughness statistically, following a microfacet-based approach, where the Normal Distribution Function (NDF) is modeled as a Beckmann distribution with average orientation β, following a V-cavity model [CT82, ON94]. The average normal orientation is thus modeled as $\beta = \arctan(R_a/l)$, where R_a is the average peak-to-valley height, and l is the profile length (both in *nm*). Note that this models roughness at the nanometer scale only; coarser features are captured by the geometry of the fibers and our specific cross sections.

Absorption Absorption inside the fiber plays a crucial role on its appearance [HM08]. The main source of absorption is the dye used to color the fiber. Thus, we compute the absorption coefficient μ_a $[m^{-1}]$ based on the amount of dye and its particular absorption as $\mu_a = \kappa\, \varepsilon$, where κ is the dye concentration $[g\ l^{-1}]$, and ε is the extinction per gram $[l\ g^{-1}\ m^{-1}]$. The latter is given by $\varepsilon = \varepsilon_m\, w_m^{-1}$, being ε_m the molar extinction coefficient in $[l\ mol^{-1}\ m^{-1}]$, and w_m the molar weight of the dye $[g\ mol^{-1}]$.

We model the dye concentration κ as a function of the fibers' density ρ $[g\ l^{-1}]$ (see Table 1), and the *Depth of Shade* (DoS) ζ, as $\kappa = \rho\zeta$. The DoS ζ is a quantity used in industry for controlling the saturation of dyed cloth, which is the ratio of grams of dye to grams of fiber (ranging from 0.1% for pale shades to 4% for deep shades [Nee01]). Note that at such small dye concentrations the impact of the dye on other optical properties of the fiber is minimal [HM08]. We choose two of the most common dyes suitable for a very wide range of commercial fabrics (reactive and disperse). Depending on their chemical and physical properties, some dyes are more suitable to be used for different kinds of fabrics: reactive dyes, which are mainly used for cotton, silk and wool, have an extinction coefficient ε ranging from 0.005 to 0.0158 $[l\ mg^{-1}\ cm^{-1}]$; disperse dyes, often used for polyester and other synthetic fabrics, have much higher extinction values, ranging from 0.045 to 0.246 [OEA*14, HHR15]. Figure 5 shows the effect of the DoS on a fiber of silk; it does not have a large effect on the color of an individual fiber, however its effect accumulates and becomes visible as it interacts with all the fibers in the cloth.

3.2. Obtaining the BCSDFs

Since no existing analytical BCSDF model can represent the complex high-frequency, anisotropic features of light transport in realistic fibers, we opt for precomputing light transport under different view and light directions, and tabulate this information to be used directly as a BCSDF.

We place a single straight fiber lit by a beam of light whose width equals the projected area of the cross section in the incoming direction. We consider an infinitesimal longitudinal patch, and adopt a far-field approximation of the BCSDF, a suitable approximation that has been shown to introduce a very low error [ZW07]. This setup allows us to simplify the eight dimensional BCSDF $f(\mathbf{x}_i, \omega_i, \mathbf{x}_o, \omega_o)$, with $\mathbf{x}_i$ and ω_i ($\mathbf{x}_o$ and ω_o) the incoming (outgoing) point and direction, respectively, into a four-dimensional BCSDF $f(\omega_i, \omega_o)$.

We discretize the angular domain in 2° intervals, which our tests showed to be enough to capture the sharpest illumination features due to direct reflection and caustics (present in polyester and silk). This results into an angular resolution of 180×90 in $\langle \phi, \theta \rangle$, for a total of $(180 \times 90)^2$ combinations of ω_i and ω_o. For each light direction, we shoot sixteen million photons from the light, and simulate their random walk as they interact with the fiber. These photons are collected in an infinite sphere bounding the fiber, as a function of $\omega_o = \langle \phi_o, \theta_o \rangle$, using the irradiance meter sensor in Mitsuba [Jak10]. We compute a two-dimensional slice of our 4D function for each incoming light direction. Our final BCSDF $f(\omega_i, \omega_o)$ is characterized by the fiber's parameters (cross section, size, index of refraction, surface roughness, dye used, and depth of shade), and is stored as a 4D table which is accessed directly in rendering time. We use the same approach for computing the directionally resolved fiber projected area $A(\omega_o)$, which will be used later for rendering (see Section 5). The average precomputation time and storage cost for each type of BSCDF is listed in Table 2. Our BCSDFs are publicly available at online[†].

4. Analysis & Discussion

Far-field assumption We assume that light interactions occur at the same differential point $\mathbf{x}$ in the fiber, which allows us to reduce the dimensionality of the BCSDFs to four dimensions. We also leverage this assumption to consider that the fiber is *locally* straight, homogeneous, and has the same cross section in all cases but wool, similar to most previous works on hair rendering [MJC*03, dFH*11, YTJR15]. This is a reasonable simplification given the small diameter of the fibers, in general much lower

† http://giga.cps.unizar.es/~ajarabo/pubs/clothEGSR17/data/

Type	Average Cost	Resolution (ω_i,ω_o)	Storage BCSDF	Total Storage
Polyester	7 min	45×1, 90×180	2.7 MB	5.56 MB
Silk	360 min	45×180, 90×180	500.5 MB	1001 MB
Cotton	420 min	45×180, 90×180	500.5 MB	1001 MB
Wool	900 min	90×180, 90×180	1001 MB	2002 MB

Table 2: *Average computation and storage cost for each of the four types of fiber considered in this work. The computation cost is affected both by the complexity of the geometry modeling the fibers, and the number of angular measurements. For rotationally symmetric fibers, such as polyester, very few angular samples are needed to characterize the full BCSDF. Fibers with longitudinal symmetry (silk, cotton) require half the measurements than wool. The total size of the BCSDF (in 32 bits floats for a monochromatic BCSDF) is directly proportional to the total resolution of the BCSDF. Finally, note that in addition to the BCSDF we also store the tabulated CDF for sampling, and the directionally-resolved albedo $\Lambda(\omega_o)$ and fiber's projected area $A(\omega_o)$.*

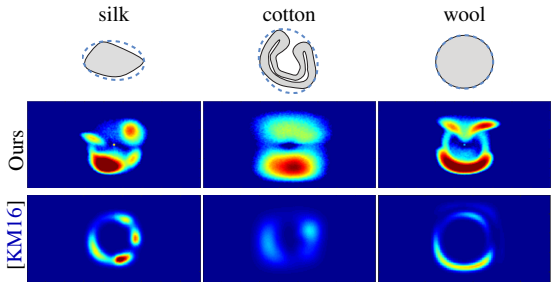

Figure 6: *Comparison between our BCSDFs (top) and the results predicted by Khungurn and Marschner's elliptical fiber model [KM16] (bottom), for fibers of silk, cotton and wool, illuminated by a beam of light with incoming direction $\theta_i = 45°$. We use the best physical fit of the elliptical model, by setting the same or closest fiber parameters - roughness, bounding ellipse and diameter, cuticle slope, etc.- to match the fiber's real parameters (bounding ellipses are rotated accordingly). Elliptical cross sections are unable to capture the complexity of realistic fiber reflectances.*

than the fibers' curvature, and assuming that the fiber's cross section and twisting varies slowly along the longitudinal axis with respect to the path length.

Comparison to elliptical fiber models Most previous fiber reflectance models have assumed circular, or moderately elliptical, cross sections [ZW07, dFH*11, YTJR15, KSZ*15]. Recently, Khungurn and Marschner [KM16] presented a fiber model supporting elliptical cross sections of arbitrary eccentricity. We compare against this model in Figure 6, by adjusting their elliptical cross section to fit ours as closely as possible and using real optical parameters. As the figure shows, even an advanced elliptical fiber model is unable to represent the rich and complex outgoing radiance field of natural fibers. Moreover, even in fibers with an actual elliptical cross section, such as wool, the complex patterns in the reflectance due to the tilted cuticles are better approximated with our model. Finally, the complexity of the azimuthal scattering component requires costly numerical integrations that cannot be performed on the fly during rendering; therefore we rely on precomputed tabulated data, similar to most current models, to produce highly accurate results.

Geometric optics assumption Our computation setup used to generate the BCDSFs (Section 3.2) is based on geometric optics. This means that wave effects such as polarization are not taken into account. However, given that even for polyester the surface is not a perfectly smooth dielectric, the degree of polarization introduced by Fresnel reflection is small, and its impact on the final image would be minimal. In addition, most cloth fibers present a small amount of birefringence [WW08], specially polyester (see Table 1). We assume isotropic dielectrics, and set an average index of refraction. Our model does not account for diffraction, which will probably appear due to the small fiber's cross section and geometric features. It is unclear how much diffraction would impact the BCSDF, although its effect will probably be slightly masked by the surface roughness and the medium absorption. Finally, some dyes may present fluorescent appearance. We assume only elastic scattering (i.e. with no energy transfer between wavelengths [GSMA08]), although a more sophisticated model could include a bispectral BCSDF, similar to the bispectral BRDFs [HHA*10]. Although our results show improved accuracy over previous existing models, a deeper exploration on wave-related phenomena remains as future work.

5. Rendering

Our BCSDFs from Section 3.2 can be plugged in both volumetric-based and fiber-based representations of cloth [KSZ*15], with a few minor modifications. The main difference is the need of keeping track of the the full frame of the fibers, not only their direction ω_f, given the lost rotational symmetry of the cross section. This affects both the phase function f_r, as well as the fiber's projected area A_i. We define the frame centered around ω_f using the rotation angle ψ_f which defines the angle between the up-vector of the fibers frame with respect to the plane defined by ω_f and the y-axis[‡] When rendering, each fiber is assigned with an initial random rotation, as well as a BCSDF from our dataset. Both values are uniformly sampled from $[0, 2\pi)$ and our set of BCSDFs, respectively.

Including fiber's rotation ψ_f is straight forward when the fibers are represented by explicit geometry in the form of curves. For the volumetric approach, we build upon the anisotropic radiative formulation by Jakob et al. [JAM*10], where the incoming radiance at $\mathbf{x}$ in direction ω_o is:

$$L(\mathbf{x}, \omega_o) = \int_0^s \Lambda(\mathbf{x}_t, \omega_o)\mu_t(\mathbf{x}_t, \omega_o)T_r(\mathbf{x}, \mathbf{x}_t)L_i(\mathbf{x}_t, \omega_o)dt, \qquad (1)$$

where $\mathbf{x}_t = \mathbf{x} - \omega_o t$, $\Lambda(\mathbf{x}_t, \omega_o)$ and $\mu_t(\mathbf{x}_t, \omega_o)$ are respectively the directionally-resolved albedo and extinction, and $T_r(\mathbf{x}, \mathbf{x}_t)$ is the transmittance between $\mathbf{x}$ and $\mathbf{x}_t$. $L_i(\mathbf{x}_t, \omega_o)$ is the inscattered radiance at $\mathbf{x}_t$ in direction ω_o:

$$L_i(\mathbf{x}_t, \omega_o) = \int_{S^2} f_r(\mathbf{x}_t, \omega_o, \omega_i)L(\mathbf{x}_t, \omega_i)d\omega_i, \qquad (2)$$

[‡] When ω_f is aligned to the y-axis, we compute the rotation based the plane defined by ω_f and the x-axis.

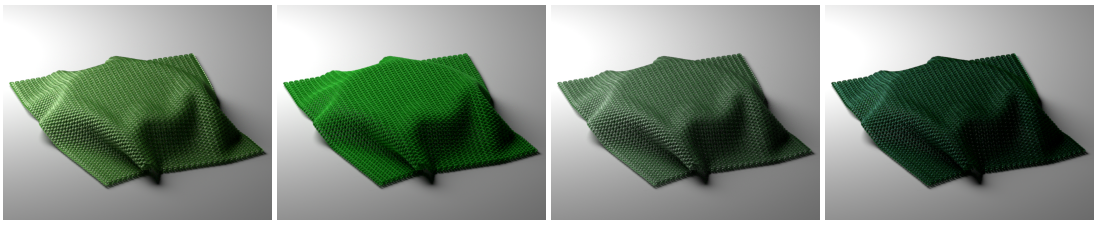

Figure 7: *Volumetric renders of a knitted stockinette fabric, where each yarn has one ply and 60 fibers, and a twist of five turns per cm, with fiber types (from left to right): cotton, polyester, silk and merino wool. All fibers are rendered with the same DoS. The almost perfectly dielectric polyester fiber produces a highly saturated fabric since very few light is directly reflected out, while the silk cloth has a clear white specular reflection that previous approaches [KSZ*15] are unable to capture. Given that wool fibers are significantly wider than the rest, for the same DoS wool fibers absorb a larger amount of light.*

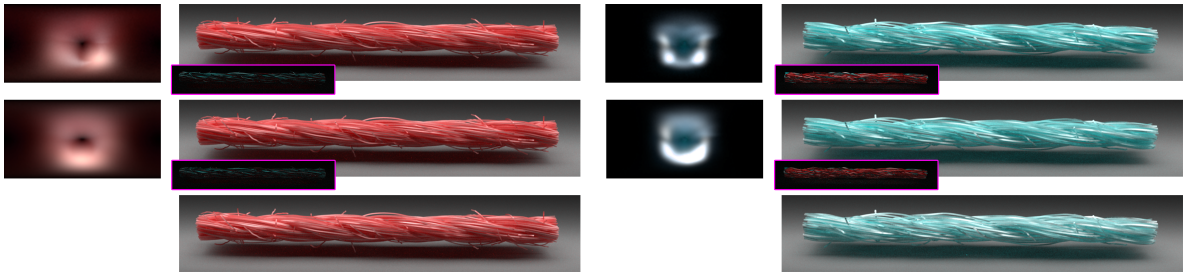

Figure 8: *Renders of cotton (red) and silk (green) yarns, captured by Zhao et al. [ZLB16]. From top to bottom, using 1) only one of our BCSDFs for every fiber, with varying cross section orientation per fiber; 2) a precomputed average of 15 and 8 BSDFs of cotton and silk, respectively; and 3) five of our BCSDFs randomly distributed among the fibers. Differences between 3), and 1) and 2) are shown in the insets (3x scaled for a better visualization).*

with f_r being the normalized phase function at $\mathbf{x}_t$, $L(\mathbf{x}_t, \omega_i)$ represents the incoming radiance at point $\mathbf{x}_t$ from direction ω_i, and S^2 is the spherical domain. We include the fiber's rotation ψ_f into the extinction $\mu_t(\mathbf{x}_t, \omega_o)$ by approximating it as:

$$\begin{aligned}\mu_t(\mathbf{x}, \omega_o) &\approx \frac{1}{V}\sum_{i=1}^{N} A_i(\omega_o')\sin(\omega_o, \omega_{f,i}) \\ &\approx \frac{N}{V}\overline{A}(\omega_o')\sin(\omega_o, \overline{\omega_f}),\end{aligned} \tag{3}$$

where N is the number of fibers falling into a voxel and V is the voxel's volume, $A_i(\omega_o')$ and $\overline{A}(\omega_o')$ are the projected cross section of fiber i and the mean projected cross section of all N fibers in direction $\omega_o' = R_f(\omega_o)$, which is the outgoing direction transformed to match the frame of the fibers. $\omega_{f,i}$ and $\overline{\omega_f}$ are the direction of fiber i and the fibers' mean direction. Note that we approximate both the distributions of fibers directions ω_f, rotations ψ_f and projected cross sections $A(\omega_o)$ using their respective mean value. The albedo $\Lambda(\mathbf{x}_t, \omega_o)$ is computed analogously.

Implementation details We implemented our BCSDFs in the physically-based renderer Mitsuba [Jak10] as specialized BSDF and phase functions, fed in both cases with the tangent frame defined by the fibers direction ω_f and rotation ψ_f. We tabulate the BCSDFs, and their CDFs for efficient sampling; the BCSDFs are normalized to one, with a separated table coding the directionally-varying albedo. We also tabulate the projection of the fibers cross section $A(\psi_f)$. The total memory cost of each of these tabulations can be found in Table 2. We do not use any compression for the BCSDFs, although standard compression techniques for high-dimensional data (e.g. tensor decomposition [RK09]) could be applied to significantly reduce the memory cost. To account for inter-fiber variability we randomly assign to each fiber a fixed cross section from our database, which spins with the fiber's local frame; we assume that this cross section does not vary along the fiber. Introducing geometrical variability along the fiber is an interesting avenue of future work.

6. Results

We demonstrate the use of our BCSDFs with the two main types of representations for cloth: volumetric and explicit fibers geometry. We use the former to render cloth garments illustrating the effect of our BCSDFs on the macroscopic appearance of cloth, and explicit fiber representations for rendering small yarns showing very detailed, close shots. We generate the volumetric garments using the work of Lopez-Moreno et al. [LMMCO15] over simulations at the yarn level [CLMMO14, CLMO15]. Figure 1 and Figure 7 show examples on the macroscopic effect on the cloth appearance of an accurate BCSDF. In particular, Figure 7 shows the exact same knitted pattern rendered using our four types of BCSDFs, keeping the rest of the parameters constant. Significant differences on the overall appearance of the garment can be found between each type of fiber.

Effect of average BCSDFs The effect of a single, detailed high-frequency scattering function can be downplayed due to the mul-

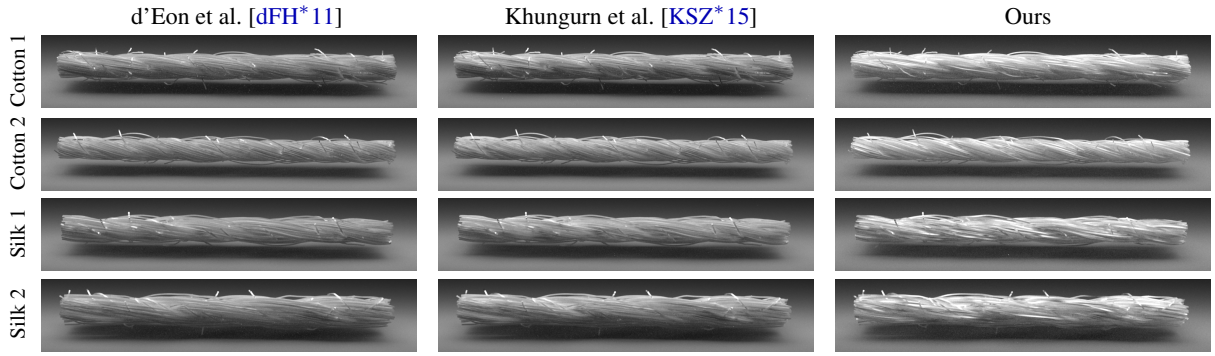

Figure 9: *Comparison between renderings of the same base fibers using the models of d'Eon et al. [dFH*11] and Khungurn et al. [KSZ*15] and our model. We fit these parametric models to match our cotton and silk BCSDFs as close as possible. The parameters of the fits, as well as our BCSDFs, can be found in Figure 12.*

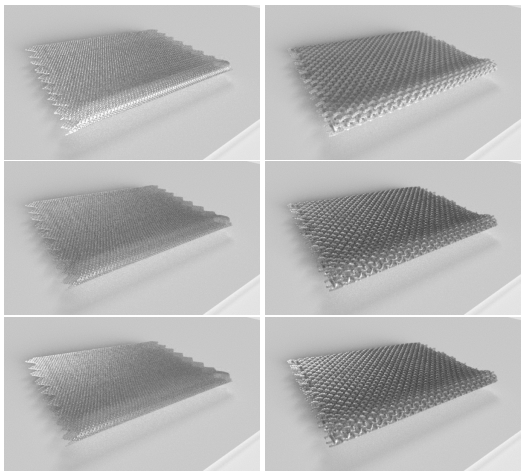

Figure 10: *Comparison between our BCSDFs (top), and the scattering models of d'Eon et al. [dFH*11] and Khungurn et al. [KSZ*15], fitted to match our BCSDFs (see Figure 12), for silk (left) and cotton (rigth) garments, rendered using a volumetric representation of cloth.*

tiple bounces in the volume, as well as by the multiple individual fibers with different BCSDFs falling in a single pixel (or voxel in a volumetric representation). In Figure 8 we investigate the effect of having a single BCSDF for all fibers in a yarn, an average BCSDF, and different BCSDFs for each fiber in the yarn. As expected, the most realistic scenario (different BCSDFs for each fiber) introduces the largest variability in terms of specular reflections, leading to a more detailed appearance. This confirms that, for very detailed shots we need to preserve the variability on the fibers BCSDFs to obtain optimal results. However, even the less detailed scenario (the average BCSDF) preserves the overall look of the BCSDFs, including an anisotropic look, which suggests that even in a convoluted volumetric rendering the final look will still vary when using detailed BCSDFs rather than parametric simplified models. In the following, we investigate this in more detail.

Figure 11: *Renders of virtual replicas of the* Gütermann *sweing yarns described in Table 3. From left to right, and top to bottom, the yarns are Skala360 (polyester), ORA 120 (polyester), CNe 50 (cotton), and S 303 (silk), with varying DoS.*

Comparison with parametric models Figure 9 compares the resulting appearance of rendering four high-quality yarns from [ZLB16] using our BCSDFs and two state-of-the-art BCSDF models [KSZ*15, dFH*11] fitted numerically to our BCSDFs (see resulting BCSDFs and fitted parameters in Figure 12). Given the non-linearity of volumetric scattering, small differences in the fit result in very different appearances: this is specially visible in the specular reflections, where current parametric methods are unable to match the anisotropic scattering found in real-world fibers, even in relatively diffuse fabrics such as cotton. This emphasizes that these models are very good for matching macroscopic appearance in top-down optimization frameworks [KSZ*15], but might lack expressivity for bottom-up definitions of appearance.

Figure 10 shows a similar comparison, this time at a macroscopic level on a volumetric representation of a full cloth garment, with fabrics made of silk and cotton, respectively.

6.1. Validation

We validate our model against sewing thread samples of 100% polyester, cotton and silk, measuring how each yarn scatters light, with different parameters to cover a reasonable range of yarn examples. We build digital replicas of these yarns (see Figure 11 for renders, and Table 3 for detailed specifications), and render them using the BCSDFs presented in Section 3.

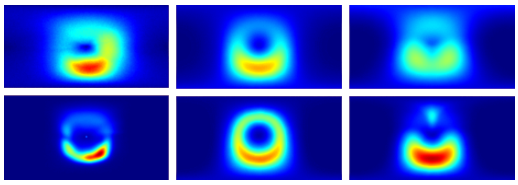

Figure 12: *Comparison between our model (left) and the parameteric fiber scattering models by Khungurn et al. [KSZ*15] (middle), and d'Eon et al. [dFH*11] (right), fitted to match our BCSDFs.* Left: *slices of our cotton (top) and silk (bottom) BCSDFs, averaged over 15 and 8 different fiber's cross section, respectively.* Center: *numerical fit for the BCSDF of Khungurn et al. [KSZ*15], with parameters (cotton, silk):* $C_R = 0.001, 0.1$, $C_{TT} = (0.5, 0.25)$, $\beta_R = (32°, 8°)$, $\beta_{TT} = (16°, 16°)$, $\gamma_{TT} = (57°, 46°)$. Right: *numerical fit for d'Eon et al.'s BCSDF [dFH*11], with parameters* $\beta = (20°, 13°)$, $IOR = (1.55, 1.55)$, $\mu = (0.1, 0.1)$.

Sample	Composition	Fiber Length	Twist	Fibers/ply	Plys
Skala 360 (*)	Polyester	continuous	5	24	1
ORA 120	Polyester	3 - 4	8.8	90	2
CNe 50 (*)	Cotton	3 - 4	12.8	70	3
S 303 (*)	Silk	5 - 8	9	90	3

Table 3: *Specifications of the set of* Gütermann *sewing yarns rendered in Figure 11. For completeness we also include the* dtex $[g/10000m]$ *measurement, which is a value typically used in industry, being from top to bottom: 74 dtex × 1; 140 dtex × 2; 90 dtex × 3; 90 dtex × 3.* Scala360, CNe 50 *and* S 303 *are used for validation of our model (Section 6.1).*

Acquisition setup We capture the reflectance of the yarns using a controlled setup at the optics laboratory. The light source is a 633 nm He-Ne laser, with a spatial filter to produce a clean Gaussian beam. The spatial filter assembly consists of a microscope objective, a pinhole aperture, and a collimating/focusing lens. An iris diaphragm is placed before the photodetector to limit its aperture acceptance to $\approx$ 10 mrad. The photodetector is a silicon PIN-photodiode with conventional transimpedance amplifier circuit, mounted on a goniometer, providing a measurement range of 360°. Since the laser beam is constant, it needs to be modulated by an optical chopper. Also, a lock-in amplifier is referenced to the operating frequency of the modulator to discard ambient light and improve the SNR allowing to extract the signal in the noisy environment. This is done by a data acquisition module connected to a computer with a lock-in amplifier algorithm [Bur05].

Measurement repeatability is over 0.5%. Figure 13, a shows photographs of the full measurements setup. Note that two different apparatus were needed for holding the yarn vertically (Figure 13, b) and horizontally (Figure 13, c). Yarns were carefully attached to the holders with a soft tension to avoid appearance variations due to stretching or shearing.

Discussion Following Sadeghi et al. [SBdDJ13], we plot the light scattered by yarns in the longitudinal axis θ (Figure 14). These plots compare the reflectances from measurements against the simulated scattering of the virtual replicas. Given the inherent difficulty of capturing the transmission lobe (e.g. calibrating the colli-

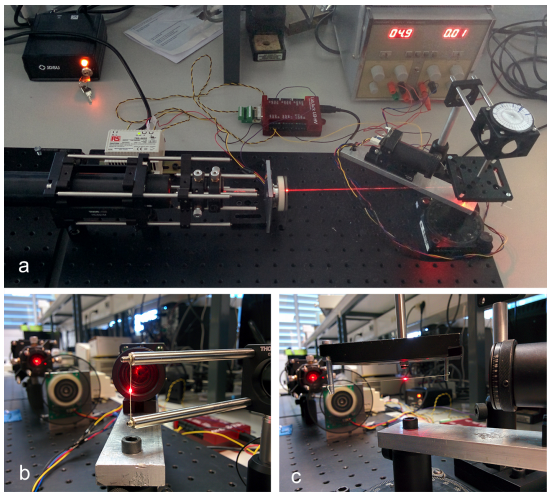

Figure 13: Top: *Full view of the measurement setup, which includes a laser light source and a photodetector mounted on a goniometer.* Bottom: *Close ups of the two different apparatus for scanning reflectance along* ψ *and* θ*, respectively.*

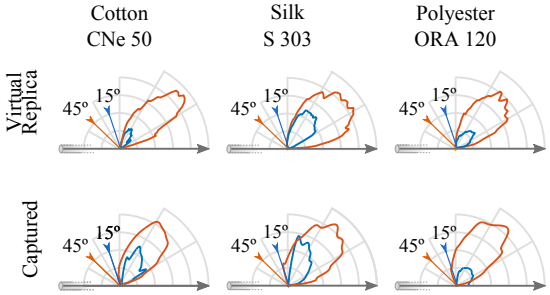

Figure 14: *Longitudinal scattering plotting (following the plots in [SBdDJ13]) of three real yarns (bottom) compared to their replicas obtained by getting the best fit approximation (top), under incoming illumination at 15° and 45° from the normal direction of the yarn. From left to right: polyester (ORA 120), silk (S 303), and cotton (CNe50) (specifications in Table 3). Abrupt changes in the measured lobes (see the 15 ° lobe of silk) are due to the unavoidable occlusions between the sensor and the laser (see Figure 13).*

mated laser beam, avoiding the saturation of the sensor) we decide to capture only the longitudinal scattering over the upper reflected directions. This allows us to observe the most notable differences in the scattering function between different pairs of fibers-yarns. Despite the limitations of the capturing setup, and the large amount of variables involved, our measurements and their virtual replicas match in terms of relative size and shape of the scattering lobes, and remain consistent between yarns with similar (but different) structure and fibers, showing interesting effects such as stronger specular reflections for fibers with higher dye concentrations.

7. Conclusions

In this paper we have focused on the definition of scattering functions for realistic cloth rendering, for both explicit and volumetric

representations. Most previous works have been directed towards accurate modeling of the mesostructure of cloth, including the type of knitting or weaving, or in formulating models for the yarns giving form to these structures. In this regard, we have gone a step further in the level of detail, by focusing on the particular scattering functions of individual fibers.

For this purpose, we have left behind common assumptions from previous fiber scattering models, such as considering fibers as cylinders with circular cross section and, together with physically-based optical parameters directly related with the fabrication properties of the fiber, developed a bottom-up approach for defining the appearance of cloth in a predictive manner. In this regard, ours is the first appearance model for fibers accounting for such detailed input. We have shown that the scattering of individual fibers is important for defining the appearance at detailed shots, and analyzed the emerging effect of these different scattering functions on cloth appearance. Further on, we have shown the limitations of previous fiber models on describing the complex features exhibited by the BCSDF of realistic fibers.

While our work is, to our knowledge, the most detailed on defining the reflectance field of cloth fibers, several assumptions have been made to build our model. The main one is related to the geometric optics assumed on the definition of the BCSDF: while the obtained results are sound and agree with the scattering acquired from measured real-world fibers, diffraction would be expected to appear when light interacts with very thin fibers. While previous work has shown that ray-optics are a good model for closely approximating complex electromagnetic phenomena at the diffraction limit (e.g. [SML*12]), it is unclear up to what extent diffraction would affect our model, although the fiber's surface roughness and medium absorption are likely to slightly reduce its effect. Investigating the wave-based phenomena, and whether it can be approximated using data processing as in previous work [SML*12, DWMG15] are interesting avenues for future work. In this context, other effects such as birefringence and fluorescence are also expected to play an important role on fibers appearance.

Despite these limitations our work has shown that more accurate physically-based BCSDFs have an important impact on the appearance of cloth. We believe that, given that rendering highly realistic cloth is a matter of subtle but important details, the approach proposed in this work is a promising path for higher-quality predictive cloth rendering.

Acknowledgements

We want to thank Gabriel Cirio and Rosa Sánchez for the cloth models, Carlos Heras, Iñigo Salinas, and Ignacio Garcés for their help with the capturing setup, Miquel Rius from Gütermann for providing the real yarn samples and manufacturing details, and Julio Marco, Adolfo Muñoz, Sandra Malpica and Miguel Galindo for their help at different stages of the project. This research has been funded by the European Research Council (ERC Consolidator Grant, ref. 682080, and ERC Proof-of-Concept Grant, ref. 713742), DARPA (project REVEAL), and the Spanish Ministerio de Economía y Competitividad (projects TIN2016-78753-P, RTC-2016-5122-5 and TIN2015-70799-R). C. Aliaga and J. López-Moreno were additionally supported by a PhD grant from Gobierno de Aragón and a Juan de la Cierva fellowship, respectively.

References

[AYMT02] ASLAN M., YAMADA J., MENGUC P., THOMASSON A.: Radiative properties of individual cotton fibers: Experiments and predictions. In *8th AIAA/ASME Joint Thermophysics and Heat Transfer Conference* (2002), p. 3325. 3

[AYMT03] ASLAN M., YAMADA J., MENGÜÇ M., THOMASSON J.: Characterization of individual cotton fibers via light-scattering experiments. *Journal of thermophysics and heat transfer 17*, 4 (2003). 3

[Bur05] BURDETT R.: Amplitude modulated signals: The lock-in amplifier. In *Handbook of Measuring System Design* (2005), John Wiley & Sons, Ltd. 9

[CBTB16] CHIANG M. J.-Y., BITTERLI B., TAPPAN C., BURLEY B.: A practical and controllable hair and fur model for production path tracing. *Computer Graphics Forum 35*, 2 (2016). 3

[CLMMO14] CIRIO G., LOPEZ-MORENO J., MIRAUT D., OTADUY M. A.: Yarn-level simulation of woven cloth. *ACM Trans. Graph. 33*, 6 (2014). 7

[CLMO15] CIRIO G., LOPEZ-MORENO J., OTADUY M. A.: Efficient simulation of knitted cloth using persistent contacts. In *Eurographics Symposium on Computer Animation* (2015), pp. 55–61. 7

[CT82] COOK R. L., TORRANCE K. E.: A reflectance model for computer graphics. *ACM Trans. Graph. 1*, 1 (1982). 5

[dFH*11] D'EON E., FRANCOIS G., HILL M., LETTERI J., AUBRY J.-M.: An energy-conserving hair reflectance model. *Computer Graphics Forum 30*, 4 (2011). 3, 5, 6, 8, 9

[DKP14] DÍAZ A., KATSARAVA R., PUIGGALÍ J.: Synthesis, properties and applications of biodegradable polymers derived from diols and dicarboxylic acids: From polyesters to poly (ester amide) s. *International Journal of Molecular Sciences 15*, 5 (2014). 3

[DVGNK99] DANA K. J., VAN GINNEKEN B., NAYAR S. K., KOENDERINK J. J.: Reflectance and texture of real-world surfaces. *ACM Trans. Graph. 18*, 1 (1999). 2

[DWMG15] DONG Z., WALTER B., MARSCHNER S., GREENBERG D. P.: Predicting appearance from measured microgeometry of metal surfaces. *ACM Trans. Graph. 35*, 1 (2015). 5, 10

[GHR97] GRASSO M. M., HUNN B. D., REWERTS A. M.: Effect of textile properties in evaluating a directional shading fabric. *Textile research journal 67*, 4 (1997), 233–247. 3

[GK81] GILLBERG G., KEMP D.: Surface characterization of polyester fibers. *Journal of Applied Polymer Science 26*, 6 (1981). 4

[GSMA08] GUTIERREZ D., SERON F., MUÑOZ A., ANSON O.: Visualizing underwater ocean optics. *Computer Graphics Forum 27*, 2 (2008). 6

[HDCD15] HEITZ E., DUPUY J., CRASSIN C., DACHSBACHER C.: The SGGX microflake distribution. *ACM Trans. Graph. 34*, 4 (2015). 2

[HHA*10] HULLIN M. B., HANIKA J., AJDIN B., SEIDEL H.-P., KAUTZ J., LENSCH H. P. A.: Acquisition and analysis of bispectral bidirectional reflectance and reradiation distribution functions. *ACM Trans. Graph. 29*, 4 (2010). 6

[HHR15] HAQUE A. N. M. A., HANNAN M., RANA M. M.: Compatibility analysis of reactive dyes by exhaustion-fixation and adsorption isotherm on knitted cotton fabric. *Fashion and Textiles 2*, 1 (2015). 5

[HM08] HEARLE J. W., MORTON W. E.: *Physical properties of textile fibres*. Elsevier, 2008. 4, 5

[HSEMN09] HAMZA A., SOKKAR T., EL-MORSY M., NAWAREG M.: Automatic determination of refractive index profile of fibers having regular and/or irregular transverse sections considering the refraction of light rays by the fiber. *Optics Communications 282*, 1 (2009). 3

[IM12] IRAWAN P., MARSCHNER S.: Specular reflection from woven cloth. *ACM Trans. Graph. 31*, 1 (2012). 2

[Jak10] JAKOB W.: Mitsuba renderer, 2010. http://www.mitsuba-renderer.org. 5, 7

[JAM*10] JAKOB W., ARBREE A., MOON J. T., BALA K., MARSCHNER S.: A radiative transfer framework for rendering materials with anisotropic structure. *ACM Trans. Graph. 29*, 4 (2010). 2, 3, 6

[Kan07] KAN C.: Surface morphological study of low temperature plasma treated wool–a time dependence study. *Modern research and educational topics in microscopy 2* (2007), 683–689. 3

[KK89] KAJIYA J. T., KAY T. L.: Rendering fur with three dimensional textures. In *Proceedings of SIGGRAPH* (1989). 2

[KM16] KHUNGURN P., MARSCHNER S.: Azimuthal scattering from elliptical hair fibers. *ACM Trans. Graph. To appear* (2016). 2, 3, 6

[KSZ*15] KHUNGURN P., SCHROEDER D., ZHAO S., BALA K., MARSCHNER S.: Matching real fabrics with micro-appearance models. *ACM Trans. Graph. 35*, 1 (2015). 2, 3, 6, 7, 8, 9

[LMMCO15] LOPEZ-MORENO J., MIRAUT D., CIRIO G., OTADUY M. A.: Sparse GPU voxelization of yarn-level cloth. *Computer Graphics Forum* (2015). 2, 7

[LW12] LIU X., WANG F.: Visible light shielding performance of fabrics with non-circular cross section fiber. *Journal of Engineered Fabrics & Fibers (JEFF) 7*, 3 (2012). 3

[LXD08] LI Z., XING Y., DAI J.: Superhydrophobic surfaces prepared from water glass and non-fluorinated alkylsilane on cotton substrates. *Applied Surface Science 254*, 7 (2008). 4

[MH99] MAKINO T., HORIBA J.-I.: Scattering of radiation by a fiber with a rough surface. *Heat Transfer - Asian Research 28*, 4 (1999). 3

[MJC*03] MARSCHNER S. R., JENSEN H. W., CAMMARANO M., WORLEY S., HANRAHAN P.: Light scattering from human hair fibers. *ACM Trans. Graph. 22*, 3 (2003). 2, 3, 5

[MPG*16] MÜLLER T., PAPAS M., GROSS M., JAROSZ W., NOVÁK J.: Efficient rendering of heterogeneous polydisperse granular media. *ACM Trans. Graph. 35*, 6 (2016). 2, 4

[MPH*15] MENG J., PAPAS M., HABEL R., DACHSBACHER C., MARSCHNER S., GROSS M., JAROSZ W.: Multi-scale modeling and rendering of granular materials. *ACM Trans. Graph. 34*, 4 (2015). 2, 4

[Nee01] NEEDLES H. L.: *Textile fibers, dyes, finishes, and processes*. Standard Publishers Distributors, 2001. 5

[NLW*16] NAM G., LEE J. H., WU H., GUTIERREZ D., KIM M. H.: Simultaneous acquisition of microscale reflectance and normals. *ACM Trans. Graph. 35*, 6 (2016). 5

[NPH14] NAYLOR G. R., PATE M., HIGGERSON G. J.: Determination of cotton fiber maturity and linear density (fineness) by examination of fiber cross-sections. part 2: A comparison optical and scanning electron microscopy. *Textile Research Journal 84*, 18 (2014). 3

[OEA*14] OTUTU J., EFURHIEVWE E., AMERU S., OSSAI E., ET AL.: Synthesis and application of hetaryl disazo disperse dyes derived from 2-amino-5-mercapto-1, 3, 4-thiadiazole and 3-chloroaniline on synthetic polymer-fibres. *Chemistry and Materials Research 6*, 4 (2014). 5

[ON94] OREN M., NAYAR S. K.: Generalization of Lambert's reflectance model. In *Proceedings of SIGGRAPH* (1994). 5

[OTS10] OGAKI S., TOKUYOSHI Y., SCHOELLHAMMER S.: An empirical fur shader. In *ACM SIGGRAPH ASIA 2010 Sketches* (2010). 3

[PDW12] PENG B., DING T., WANG P.: Propagation of polarized light through textile material. *Applied optics 51*, 26 (2012). 3

[RGS10] RAMÍREZ F. A. M., GARCIA-SUCERQUIA J.: Optical fibre characterization through digital holographic microscopy. In *Biomedical Optics* (2010), Optical Society of America, p. JMA18. 3

[RK09] RUITERS R., KLEIN R.: Btf compression via sparse tensor decomposition. *Computer Graphics Forum 28*, 4 (2009). 7

[SBdDJ13] SADEGHI I., BISKER O., DE DEKEN J., JENSEN H. W.: A practical microcylinder appearance model for cloth rendering. *ACM Trans. Graph. 32*, 2 (2013). 2, 9

[SKZ11] SCHRÖDER K., KLEIN R., ZINKE A.: A volumetric approach to predictive rendering of fabrics. *Computer Graphics Forum 30*, 4 (2011). 2, 3

[SML*12] SADEGHI I., MUNOZ A., LAVEN P., JAROSZ W., SERON F., GUTIERREZ D., JENSEN H. W.: Physically-based simulation of rainbows. *ACM Trans. Graph. 31*, 1 (2012). 4, 10

[SPJT10] SADEGHI I., PRITCHETT H., JENSEN H. W., TAMSTORF R.: An artist friendly hair shading system. *ACM Trans. Graph. 29*, 4 (2010). 3

[SPV14] SHAH D. U., PORTER D., VOLLRATH F.: Opportunities for silk textiles in reinforced biocomposites: Studying through-thickness compaction behaviour. *Composites Part A: Applied Science and Manufacturing 62* (2014). 3

[SSK03] SATTLER M., SARLETTE R., KLEIN R.: Efficient and realistic visualization of cloth. In *Proceedings of EGSR* (2003). 2

[SZK15] SCHRÖDER K., ZINKE A., KLEIN R.: Image-based reverse engineering and visual prototyping of woven cloth. *IEEE Trans. Vis. Comp. Graph. 21*, 2 (2015). 2, 3

[SZZ12] SCHRÖDER K., ZHAO S., ZINKE A.: Recent advances in physically-based appearance modeling of cloth. In *SIGGRAPH Asia 2012 Courses* (2012). 2

[TMM09] THOMASSON J., MANICKAVASAGAM S., MENGÜÇ M.: Cotton fiber quality characterization with light scattering and fourier transform infrared techniques. *Applied spectroscopy 63*, 3 (2009). 3

[Tro84] TROTMAN E. R.: *Dyeing and chemical technology of textile fibres*. Wiley, 1984. 4

[WW08] WEIDLICH A., WILKIE A.: Realistic rendering of birefringency in uniaxial crystals. *ACM Trans. Graph. 27*, 1 (2008). 6

[WY17] WU K., YUKSEL C.: Real-time fiber-level cloth rendering. In *Proceedings of I3D* (2017). 2

[XCL*01] XU Y.-Q., CHEN Y., LIN S., ZHONG H., WU E., GUO B., SHUM H.-Y.: Photorealistic rendering of knitwear using the lumislice. In *Proceedings of SIGGRAPH* (2001). 2

[Yam02] YAMADA J.: Radiative properties of fibers with non-circular cross sectional shapes. *Journal of Quantitative Spectroscopy and Radiative Transfer 73*, 2 (2002), 261–272. 3

[YK00] YAMADA J., KUROSAKI Y.: Radiative characteristics of fibers with a large size parameter. *International journal of heat and mass transfer 43*, 6 (2000), 981–991. 3

[YKTU92] YAMADA J., KUROSAKI Y., TAKE-UCHI M.: Radiation transfer in a fibrous medium with fiber orientation. In *28th National Heat Transfer Conference and Exhibition* (1992). 3

[YTJR15] YAN L.-Q., TSENG C.-W., JENSEN H. W., RAMAMOORTHI R.: Physically-accurate fur reflectance: modeling, measurement and rendering. *ACM Trans. Graph. 34*, 6 (2015). 2, 3, 5, 6

[ZHRB13] ZHAO S., HASAN M., RAMAMOORTHI R., BALA K.: Modular flux transfer: efficient rendering of high-resolution volumes with repeated structures. *ACM Trans. Graph. 32*, 4 (2013). 2

[ZJMB11] ZHAO S., JAKOB W., MARSCHNER S., BALA K.: Building volumetric appearance models of fabric using micro ct imaging. *ACM Trans. Graph. 30*, 4 (2011). 2, 3

[ZJMB12] ZHAO S., JAKOB W., MARSCHNER S., BALA K.: Structure-aware synthesis for predictive woven fabric appearance. *ACM Trans. Graph. 31*, 4 (2012). 2

[ZLB16] ZHAO S., LUAN F., BALA K.: Fitting procedural yarn models for realistic cloth rendering. *ACM Trans. Graph. 35*, 4 (2016). 2, 3, 7, 8

[ZW07] ZINKE A., WEBER A.: Light scattering from filaments. *IEEE Trans. Vis. Comp. Graph. 13*, 2 (2007). 2, 3, 5, 6